NJC

ROYAL SOCIETY OF CHEMISTRY

PAPER

View Article Online
View Journal

Cite this: DOI: 10.1039/d0nj06095j

Synthesis of heteroleptic phosphine–copper(I) complexes: fluorescence sensing and catalytic properties†

Chen-Lin Luo,‡[a] Chu-Xing Hu,‡[a] Ping Shang,*[a] Guan-Zhao Wen,[b] Jia-Jun Zhu,[a] Ya-Hui Xuan,[a] Bang-Lian Xia,[a] Yu-Chen Liu,[a] Zi-Hao Jiang,[a] Geng Dong,[b] Wei Zhang,[c] Liu-Cheng Gui*[d] and Xuan-Feng Jiang *[ae]

Received 15th December 2020,
Accepted 1st April 2021

DOI: 10.1039/d0nj06095j

rsc.li/njc

Heteroleptic copper(I)–phosphine complexes have attracted considerable attention because of their diverse structures, and photophysical and catalytic properties. In this work, a series of heteroleptic diimine–diphosphine Cu(I) complexes (**C1–C10**) were synthesized quantitively using the designed bipyridine (**L1–L4**) and bidentate polyphosphine (**L5–L8**) as functional ligands. These mixed ligand–copper(I) complexes were fully characterized by ^{1}H and ^{13}C NMR spectroscopy, electrospray ionization mass spectrometry (ESI-MS) and elemental analysis. The detailed structures of complexes **C1**, **C2**, **C5**, **C6**, **C9** and **C10** were confirmed by single-crystal X-ray diffraction analysis. Moreover, these phosphine–Cu(I) complexes exhibited intense emissions either in the solid state or in solution under UV light excitation. The emissive complexes **C1–C4** displayed highly sensitive luminescence sensing towards silver ions in a quenching fashion (turn-off). Furthermore, all the phosphine-protected copper(I) complexes exhibited high catalytic activity towards azide–alkyne cycloaddition (CuAAC) in water.

Introduction

Cu(I) complexes have received extensive attention because of their unusual structures and intriguing properties.[1–6] Among them, heteroleptic diimine–diphosphine copper(I)-based complexes not only exhibited various structures including polynuclear clusters,[5–9] metallocycles,[10] and cages,[11] but also displayed promising applications in the fields of long-lived excited materials,[12] catalytic chemistry,[13–15] medicine[16] and so on. In these mixed-ligand cooperative coordination systems, the photophysical properties and stability of copper(I) complexes can be effectively improved by subtle structural modifications and coordination mode change of chelating diimine or phosphine ligands.[17] Therefore, in the past two decades, many efforts have been devoted to the development of stable heteroleptic Cu(I) complexes supported by mixed diimine–phosphine ligands.[1–8,18,19] In such a Cu(I)–phosphine coordination system, the structural conformation and electron-donating ability of diimine and phosphine ligands played a crucial role in achieving controlled synthesis and tunable properties of heteroleptic Cu(I) complexes.[1–10]

In this work, a series of novel diimine ligands (**L1–L4**) were rationally designed and synthesized through multi-step reactions at the bipyridine backbone (as shown in Scheme S1, ESI†). Combined with bisphosphine ligands (**L5**, POP; **L6**, dppm; **L7**, dppe; **L8**, dppp), ten heteroleptic diimine–diphosphine Cu(I) complexes (**C1–C10**) were precisely synthesized in a single step (Scheme 1). These well-defined copper(I) complexes were fully characterized by ^{1}H and ^{13}C NMR spectroscopy and mass spectrometry. The structural features of the mononuclear complexes **C1–C6** and dinuclear complexes **C7–C10** were also confirmed by X-ray single-crystal diffraction analysis. Moreover, these phosphine–Cu(I) complexes exhibit good photophysical properties either in the solid state or in solution. The heteroleptic copper(I) complexes **C1–C6** presented sensitive

[a] Key Laboratory of Green Preparation and Application for Functional Materials, Ministry of Education, Hubei Key Laboratory of Polymer Science, School of Materials Science and Engineering, Hubei University, Wuhan, Hubei, 430062, P. R. China. E-mail: pingshang02@126.com, xuanfengjiang@hubu.edu.cn
[b] School of Physics and Materials Science, Guangzhou University, GuangZhou, 510006, China
[c] Medical Informatics Research Center, Shantou University Medical College, Shantou 515041, China
[d] State Key Laboratory for the Chemistry and Molecular Engineering of Medicinal Resources, School of Chemistry & Pharmaceutical Sciences, Guangxi Normal University, Guilin, Guangxi, 541004, P. R. China. E-mail: guiliucheng2000@163.com
[e] Hubei Key Laboratory of Processing and Application of Catalytic materials, Huanggang Normal University, Huanggang, Hubei, 438000, P. R. China

† Electronic supplementary information (ESI) available. CCDC 2050236–2050238, 2050240, 2070930 and 2070931. For ESI and crystallographic data in CIF or other electronic format see DOI: 10.1039/d0nj06095j

‡ These authors contributed equally.

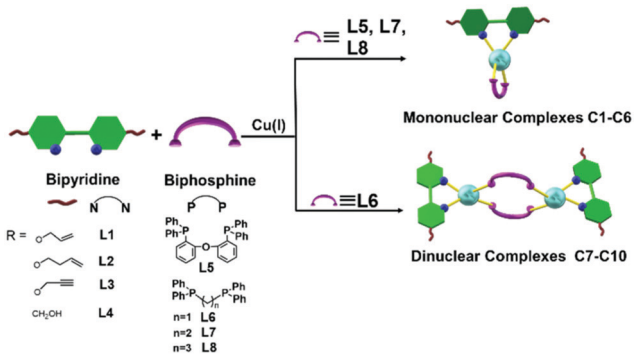

Scheme 1 The synthesis routes of the heteroleptic phosphine–copper(I) complexes **C1–C10**. The carton parts represent bipyridine and bisphosphine (green: bipyridine; purple: bisphosphine; blue ball: Cu^+ atom).

luminescence sensing towards silver ions in a quenching fashion (turn-off). Furthermore, all the phosphine-protected copper(I) complexes exhibited good catalytic activity towards azide–alkyne cycloaddition (CuAAC) performed in water.

Results and discussion

Synthesis of the ligands

Scheme 1 presents four new bipyridine and two common bisphosphine ligands used in this work. The bipyridine ligands (**L1–L4**) were synthesized using a method reported in previous studies.[16,17] Four bisphosphine ligands (**L5–L8**) were purchased from a chemical company.

Self-assembly and characterization of heteroleptic Cu(I) complexes C1–C10

A mixture of bipyridine ligand, bisphosphine and copper(I) salt ($[Cu(CH_3CN)_4]\cdot BF_4$) in equal amounts was added into 4 mL of acetonitrile solution and stirred for 24 hours at room temperature. The resulting clear solution was filtered and precipitated with 30 ml of diethyl ether. A yellow powder was afforded in quantitative yield after freeze-drying treatment. High-quality single crystals of complexes **C1–C10** were obtained by vapor diffusion of diethyl ether into their acetonitrile solution for one week.

The mononuclear Cu(I) complex **C1** was fully characterized by NMR spectroscopy, ESI-MS and X-ray crystallography. The ^1H and ^{13}C NMR spectra indicated that complex **C1** was successfully synthesized as a single highly symmetrical species. As shown in Fig. 1a and Fig. S16 (ESI†), the integration of proton signals revealed a 1 : 1 : 1 ratio between the three components, namely, the dipyridine ligand (**L1**), Cu(I) central atom and diphosphine-based ligand (**L5**). The resonance of the aromatic rings of the pyridine ligand appeared at 8.24, 7.82, and 7.46 ppm and the chemical shifts corresponding to the terminal alkene groups were also found at 5.82, 5.19, and 4.27 ppm in the upfield. Four sets of multiplets observed at 7.24, 7.13, 6.91 and 6.68 ppm can be attributed to the proton signals of the diphosphine ligand (POP). Furthermore, no remarkable signal change was observed in the temperature-dependent ^1H NMR

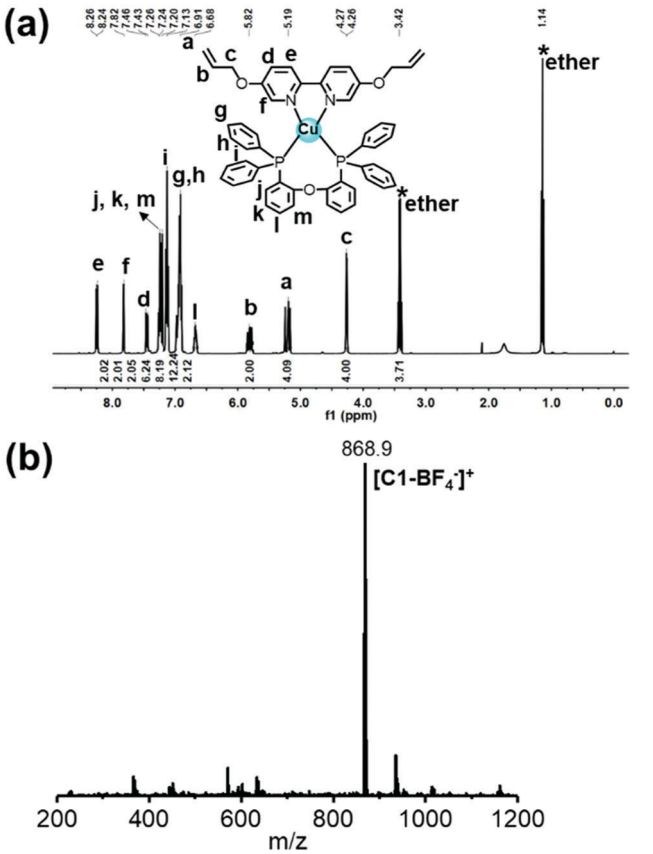

Fig. 1 ^1H NMR spectrum of **C1**·BF_4– in $CDCl_3$ at room temperature (a) and ESI-MS spectrum in acetonitrile solution (b).

spectrum, suggesting that the heteroleptic copper(I) complex **C1** has good thermodynamic stability in solution (Fig. S19, ESI†). Moreover, the formation of the heteroleptic [(POP)-Cu(bpy)]$^+$-type complex was further supported by electrospray ionization mass spectrometry (ESI-MS): 868.9 for [**C1**-BF_4^-]$^+$ (Fig. 1b). A similar procedure used for the preparation of **C1** was used to synthesize **C2–C10** (Scheme 1). The NMR and ESI-MS spectra of **C2–C10** were fully characterized and confirmed the copper(I) complex structures (Fig. S21–S49, ESI†). These experimental results indicated that the heteroleptic [(P^P)Cu(bpy)]$^+$-type complexes **C1–C10** were stable and retained complete molecular structures in solution.

Crystal structures of heteroleptic phosphine-copper(I) complexes

High-quality single crystals of complexes **C1**, **C2**, **C5**, **C6**, **C9** and **C10** suitable for X-ray crystallography were successfully grown *via* the diffusion of diethyl ether into their acetonitrile solution at room temperature. The crystal structures of complexes **C1** and **C2** are displayed in Fig. 2a and the selected structural data are summarized in Tables S2 and S3 (ESI†). The X-ray diffraction analysis revealed that **C1** and **C2** are mononuclear complexes composed of one copper(I) ion, the bipyridine ligand and the bisphosphine ligand **L5** (POP). The central copper ion adopted tetrahedral coordination conformation to interact with

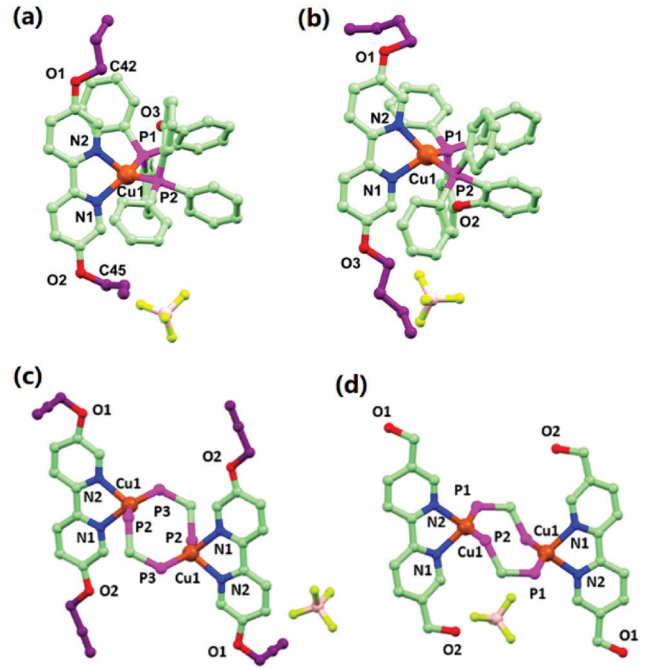

Fig. 2 Crystal structures of mononuclear complexes **C1** (a), **C2** (b), **C9** (c) and **C10** (d) drawn in the ball-stick mode. Green, carbon; blue, nitrogen; purple, phosphor; red, oxygen; brown, copper. The terminal carbon atoms at the bipyridine ligands are shown in deep violet.

two phosphine donors from the distorted organophosphorus ligand (POP) and two nitrogen atoms from the bipyridine ligands (**L1** and **L2**) forming [(POP)Cu(bpy)]$^+$-type triple-component complexes.

Taking **C1** and **C2** for example, in the distorted [(P^P)Cu(N^N)]$^+$ tetrahedral coordination moiety, the bond distances of Cu1–P2 and Cu1–N2 in complex **C1** are about 2.25 and 2.10 Å, respectively, which are slightly shorter than those found in complex **C2** (2.24 Å for Cu1–P2, 2.049 Å for Cu1–N2). The N1–Cu–N2 angles of 79.17° and 80.19° are observed in the tetrahedra of **C1** and **C2**, respectively. In a distorted eight-membered ring, the P1–Cu1–P2 angles are 112.34° and 111.97°, and the P1–Cu1–N2 bond angles in these two complexes are in the range of 101–128°. The dihedral angles of triangular planes composed of Cu1–N1–N2 and Cu1–P1–P2 are 81.27° and 81.40°, respectively (Tables S2 and S3, ESI†). These structural features indicate that the mononuclear heteroleptic complexes **C1–C4** have a similar [(P^P)Cu(N^N)]$^+$ tetrahedral coordination geometry.

In order to precisely control the structures of the heteroleptic phosphine–copper(I) complexes, a linear diphosphine ligand, **L6**, was used as a linker to assemble the dinuclear complexes **C9** and **C10** under similar conditions. Compared with the mononuclear complexes **C1–C4**, the dimeric complexes **C9** and **C10** contain two bipyridine-protected copper(I) centers doubly bridged by two polyphosphoric ligands **L6** (dppm) as depicted in Fig. 2b and Tables S6 and S7 (ESI†). In these heteroleptic di-copper(I) complexes, three components also formed two [(P^P)Cu(N^N)]$^+$ tetrahedral geometries. In **C10**, the average bond length of Cu–P is 2.24 Å and the average Cu–N bond length is 2.080 Å. The Cu(1)–P(2) and Cu(1)–P(3) bond lengths in **C9** are slightly shorter (2.247 and 2.226 Å, respectively) than those observed in the similar complex **C10**. The Cu–N bond lengths in **C9** are in the range of 2.064–2.105 Å. The N–Cu–P bond angles vary from 100.00° to 105.24°, and the N–Cu–N bond angle is 78.72° for **C9**, while the N–Cu–P bond angles for **C10** vary from 96.13° to 105.75°, and the N–Cu–N bond angle is 79.3°. The dihedral angles of Cu–N–N and Cu–P–P are 85.42° and 83.87°, respectively, which are slightly larger than those in the mononuclear complexes **C1** and **C2**. In the dinuclear complexes **C9** and **C10**, the Cu–Cu distances of two Cu(I) atoms are 4.123 and 4.393 Å, respectively.

Inspired by the structural diversity of the aforementioned Cu(I) heteroleptic complexes **C1–C2** and **C9–C10**, two linear diphosphine ligands with a longer alkyl chain (**L7**, dppe; **L8**, dppp) were reacted with copper(I) salt and bipyridine ligands (**L1–L4**) in acetonitrile solution. Interestingly, two mononuclear copper–phosphine complexes were obtained in high yields (>80%). As shown in Fig. S54 (ESI†), in complex **C5**, the copper(I) central atom coordinated with two nitrogen atoms (Cu01–N6, 2.033 Å, and Cu01–N7, 2.042 Å) and phosphine atoms (Cu01–P003, 2.2503 Å, and Cu01–P15, 2.2532 Å) in a distorted tetrahedral geometry. Similar structure and coordination moiety can be found in complex **C6** after the replacement of **L7** with the more flexible diphosphine ligand **L8** (Fig. S55, ESI†). These structural differences of complexes **C1–C10** revealed that the flexibility of diphosphine ligands plays a crucial role in the synthesis of heteroleptic Cu(I) complexes.

Spectroscopic properties

The photophysical data of the heteroleptic Cu(I)–phosphine complexes **C1–C10** are displayed in Table S6 (ESI†). The electronic absorption spectra of complexes **C1–C10** in the solid state are depicted in Fig. S104 (ESI†). Complexes **C1–C10** display intense absorption bands over a wide range from 250 to 450 nm; the lower energy bands (350–450 nm) could have possibly been caused by the exciton coupling of metal-to-ligand charge transfer (MLCT).[18–25] The mononuclear Cu(I) complexes **C1–C4** in MeCN show a similar absorption band at 310–400 nm (Fig. S106–S108, ESI†), which arises from the ILCT and π–π* charge transfer transitions. The electronic absorption spectra of the dinuclear complexes **C7–C10** in MeCN (Fig. S107 and S108, ESI†) show two absorption bands near 260–290 nm and 310–330 nm which can be attributed to the MLCT (^{1}[3d(Cu) → π*(*N*-heteroaromatic ligand)]) transitions.[23–25] Fig. 3a shows the emission spectra of complexes **C1–C10** in the solid state. With reference to the luminescence studies of heteroleptic Cu(I)–phosphide complexes reported in previous work,[26–33] the solid-state emissions of the mononuclear complexes **C1–C6** observed in the range of 556–598 nm are derived from the [(P^P)Cu(N^N)]$^+$ framework, and the origins are tentatively attributed to the triplet ligand-to-metal charge transfer (LMCT) transitions. Compared with **C1–C4**, the dinuclear complexes **C7–C10** exhibit intense solid-state emissions over a narrow range of 503–546 nm upon excitation at 384 nm and 398 nm. In CH_2Cl_2 solution, complexes **C1–C4** show emission peaks

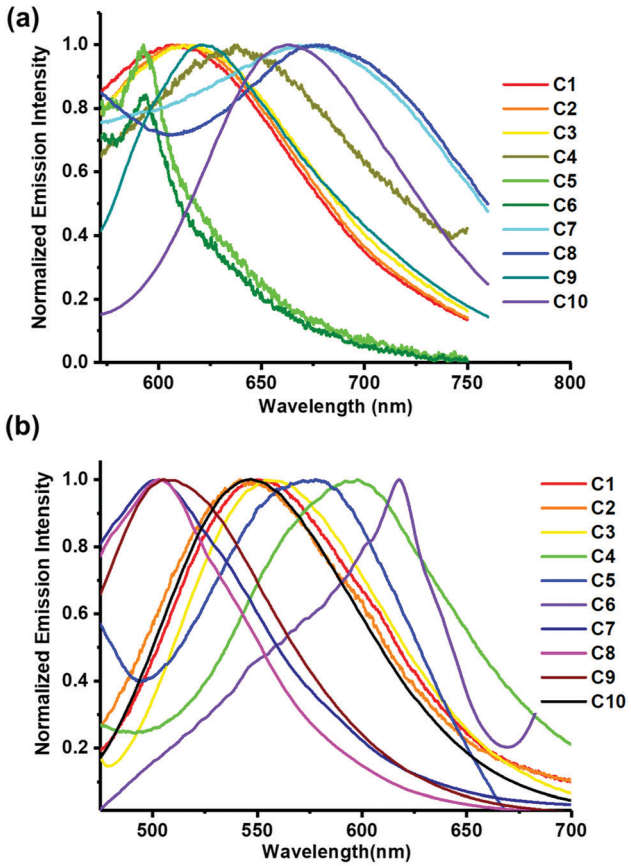

Fig. 3 (a) Emission spectra of complexes **C1–C10** in the solid state and (b) in CH_2Cl_2 solution (1×10^{-6} M) at 298 K.

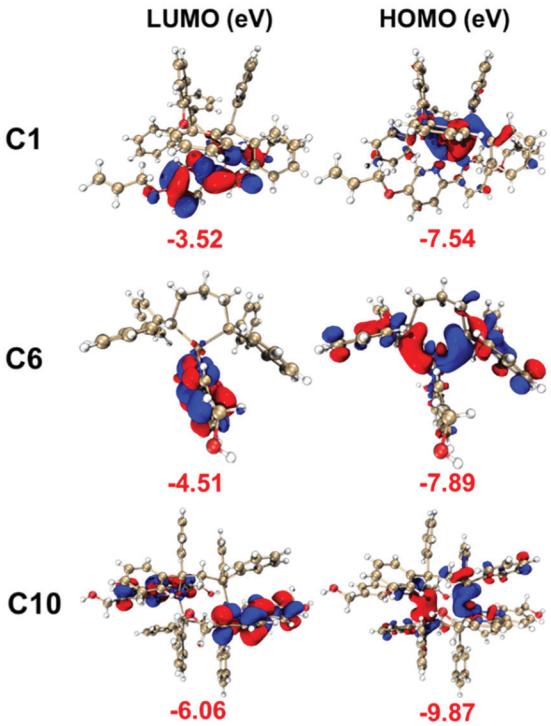

Fig. 4 Selected frontier orbitals and their energies for the mononuclear complexes **C1** and **C6**, and the dinuclear complex **C10**.

(610 nm, 610 nm, 615 nm and 640 nm) based on excitation at 421 nm, 421 nm, 415 nm and 398 nm, respectively (Fig. 3b and Fig. S71–S75, ESI†). However, **C7–C10** in CH_2Cl_2 solution show broad emission peaks at 543 nm, 560 nm, 501 nm and 543 nm, respectively. The remarkable red-shifted emission could have possibly been caused by the merely changing nature of the tetrahedron coordination geometry when the Cu(I) center interacts with different diphosphine ligands, **L5–L8**. The lifetimes and quantum yields of complexes **C1–C10** were measured and are summarised in Table S8 (ESI†). All complexes exhibit lifetimes in a broad range of 1.07–1008 μs either in the solid state or in DCM solution at room temperature, suggesting that the electron transfer originated from the triplet MLCT transitions.

In order to gain insights into the electron transfer behaviours observed in the heteroleptic complexes **C1–C10** in the solid state, the gap energy between the LUMO and HOMO was calculated using the DFT/B3LYP/Def2-SVP method. As shown in Fig. 4 and Table S9 (ESI†), the HOMO–LUMO energy gaps of the mononuclear complexes **C1** and **C6** and the dinuclear complex **C10** are 4.02, 3.38, and 3.81 eV, respectively. These theoretical calculation results indicated that electron transfer can be possibly attributed to a mixture of triplet MLCT {d(Cu) → π*[bpy]} and LLCT transitions which are in good agreement with the experimental results observed from the UV-vis absorption and solid-state emission spectra.

Silver ions are widely dispersed in industrial wastewater. Highly sensitive and selective luminescence sensing towards silver ions is still a challenging problem. However, because silver ions are luminescence-silent, ideal fluorescent probes for sensitively detecting silver ions in solution have rarely been reported to date.[22,26,27] The heteroleptic $[(POP)Cu(bpy)]^+$-type complexes **C1–C10** exhibit good stability and strong emission in solution, suggesting that these complexes can be used as potential fluorescent probes for detecting silver ions. As shown in Fig. 5, the fluorescence intensity of **C1** at 610 nm decreased gradually upon the dropwise addition of Ag^+ (from 0 to 3.4 equivalents) into the DCM solution. When the concentration of Ag^+ in the mixture solution was below 0.8×10^{-6} M, the fluorescence intensity of **C1** changed slowly. When the Ag^+ concentration reached 3.4 uM, the emission intensity is no longer significantly weakened. In order to rule out the possible interference from organic solvents, more than 4.0 equivalents of acetonitrile was added into the DCM solution of complex **C1**. The emission intensity of **C1** at 610 nm did not change remarkably, suggesting that the luminescence quenching behaviour was most likely to be caused by the strong interactions between the silver ions and complex **C1** in solution. Moreover, similar fluorescence sensing and solvent interference experiments were also carried out using complexes **C2–C8** as probes. As shown in Fig. S109–S112 (ESI†), upon the addition of silver ions, the emission intensities of **C2–C4** decreased gradually in DCM/CH_3CN solution. In contrast, the dinuclear complexes **C7–C10** did not exhibit "turn-off" fluorescence sensing towards silver ions. To gain insights into possible interaction

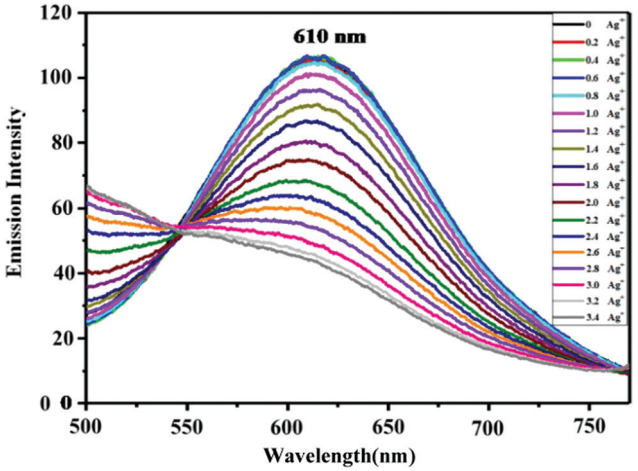

Fig. 5 Fluorescence spectra of **C1** (1×10^{-6} M) upon titration with Ag^+ ($0–3.4 \times 10^{-6}$ M) in CH_2Cl_2 solution at room temperature.

mechanisms between complexes **C1–C4** and silver ions in solution, the ^{1}H-NMR titration experiment was performed. When 10 eq. of $AgPF_6$ was added into the DCM solution of complex **C1**, the proton signals from the terminal alkene groups in the range from 5.0 to 6.2 ppm moved toward the lower field with a maximum shift of 0.7 ppm (Fig. 6). Three resonance signals from the bipyridine ligand **L1** in the range of 7.5–8.3 ppm shifted to one set of multiple signals at 7.48 ppm. Furthermore, five sets of chemical shifts in the range from 6.7 to 7.5 ppm, attributed to protons from the POP ligand **L5**, changed to three dominant signals at 6.8, 7.1, and 7.3 ppm. Based on these results, we speculated that the silver ions could have possibly interacted with complex **C1** through multiple $Ag^+\cdots\pi$ interactions in solution. These weak interactions interfered with the metal-to-ligand charge transfer behaviour between the copper center and the bipyridine and diphosphine ligands, leading to luminescence quenching.

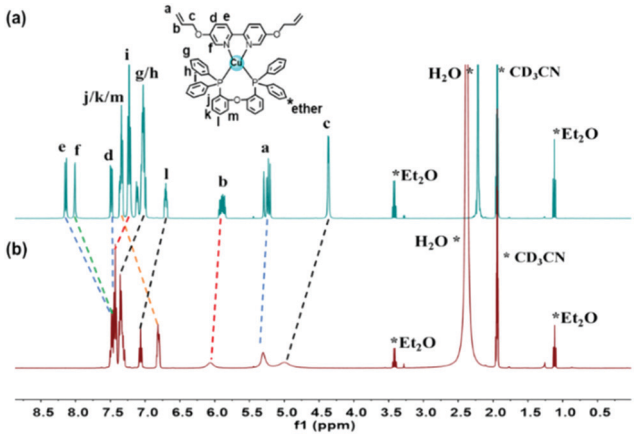

Fig. 6 ^{1}H-NMR spectra of the mononuclear complex **C1** before (a) and after the addition of silver ions (4 eq.) in CD_3CN. The dashed lines show the change in chemical shifts before and after complexation.

Catalytic activity toward the CuAAC reaction in water

Metal-catalyzed azide–alkyne cycloaddition reactions are widely used in organic synthesis, medicinal chemistry, high polymer chemistry and biological coupling.[25] In particular, Cu(I) complexes exhibited high catalytic activity towards azide–alkyne cycloaddition reactions (CuAAC) carried out in aqueous solutions.[26–28] However, a few heteroleptic Cu(I) complexes stabilized with diimine–polyphosphine ligands have been used as efficient catalysts for CuAAC reactions carried out in water under mild conditions.[29–35] As shown in Table 1, seven aromatic alkynyl-based substrates **1a–1g**, respectively, reacted with benzyl azide (**2a**) at 80 °C for 8 h. The experimental yields were calculated based on the target triazolyl compounds **3a–3g** purified by column chromatography (DCM as the eluent). Alkyne substrates **1a–1c** with electron-donating groups displayed good reactivity towards benzyl azide, and the highest yields of the corresponding triazole reached 97% (**3b**) and 95% (**3d**). In order to study the circulation of the catalyst, the catalytic yield remains 60% after recycling four times in the reaction of phenylacetylene (**1a**) with benzyl azide (**2a**). All the triazolyl compounds **3a–3g** were fully characterized by NMR spectroscopy and mass spectrometry (Fig. S116–S134, ESI†). Based on previous studies,[32–35] as shown in Fig. S135 (ESI†), we proposed a mechanistic pathway for the CuAAC reaction catalyzed by heteroleptic complexes. The azide and alkyne substrates possibly coordinate with the copper(I) atom *via* Cu–N

Table 1 The CuAAC reaction catalyzed by complex **C1** at 80 °C

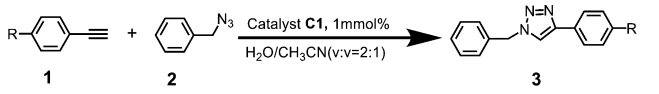

1 2 3

Entry	Alkyne	Azide	Product[a]	Yield[b] (%)
1	1a		3a	96
2	1b		3b	97
3	1c		3c	92
4	1d	2a	3d	95
5	1e		3e	85
6	1f		3f	88
7	1g		3g	90

[a] Reaction conditions: azide (0.1 mmol), alkyne (0.11 mmol), complex **C1** as catalyst (1 mmol %), water (2 mL), CH_3CN (1 mL), 80 °C, 8 h. [b] The isolated product yield was calculated through recrystallization from the reaction solution and determined using ^{1}H NMR and ESI mass spectra.

and Cu–C bonds, leading to the formation of intermediates B and C, respectively. After the [2+3]-cycloaddition and the cleavage of the C–Cu bond, the triazole product was produced and separated from intermediate D.

Conclusions

A series of bipyridine ligands with various side chains were synthesized and used to synthesize ten diphosphine-supported heteroleptic complexes **C1–C10**. The mononuclear conformation was changed to dinuclear by replacing the semi-rigid bisphosphine ligand POP with a flexible linear linker, Dppm, in the assembly process. These discrete triple-component complexes were fully characterized by NMR spectroscopy, ESI-MS and X-ray crystallography. These heteroleptic Cu(I) complexes exhibited good stability and intense wide-range emissions either in the solid state or in solution. The mononuclear complexes **C1–C4** with modified bipyridine displayed ''turn-off'' fluorescence sensing towards silver ions in DCM/CH_3CN solution. The possible luminescence probing mechanism was proposed based on the NMR titration experimental results. Furthermore, all these water-stable phosphine–copper(I) complexes exhibit high catalytic activity towards the CuAAC reaction in water/CH_3CN solution.

Experimental section

All reactions and manipulations were performed under an atmosphere of prepurified nitrogen using Schlenk techniques. All the organic solvents were purchased from a commercial chemical company and were used after being distilled over 4 Å molecular sieves under an argon atmosphere. All other chemicals were used as received without any further purification. NMR spectra were recorded using either a Bruker AVIII 400 MHz spectrometer or a Bruker AVIII 500 MHz spectrometer and referenced to residual solvent peaks. The working frequencies were 400 or 500 MHz for ^{1}H and 100/125 MHz for ^{13}C. The fluorescence spectral analyses were carried out using Edinburgh FLS980 and Gangdong FL-320 spectrometers. The X-ray diffraction single-crystal data of the Cu(I)–POP complexes **C1–C6** and Cu(I)–Dppm complexes **C7–C10** were collected using a Bruker D8 Venture APEX II CCD single-crystal diffractometer.

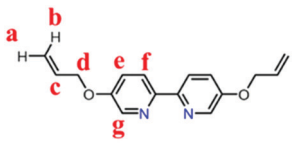

L1

Synthesis of ligand L1

(2,2'-Bipyridine)-5,5′-diol (100 mg, 0.53 mmol), K_2CO_3 (2.50 g, 18.12 mmol), KI (20 mg, 0.12 mmol) and allyl bromide (0.8 mL, 9.26 mmol) were dissolved in dry THF (20 mL) in a sealed tube. The mixture was stirred at 85 °C for 48 hours. Next, the solution was concentrated under reduced pressure. The afforded solid was dissolved in CH_2Cl_2 and washed with water, then brine, dried (Na_2SO_4), and the solvent was evaporated in a vacuum. Flash chromatography (SiO_2, AcOEt: light petroleum) afforded **L1** as a pale-yellow solid (80.50 mg, 0.30 mmol, 57%). ^{1}H NMR (500 MHz, chloroform-*d*) δ 8.33 (d, J = 3.0 Hz, 2H, H^g), 8.22 (d, J = 8.8 Hz, 2H, H^f), 7.30 (d, J = 3.0 Hz 2H, H^e), 6.07 (brs, 2H, H^c), 5.47(d, J = 18.4 Hz, 2H, H^b), 5.35 (d, J = 11.4 Hz, 2H, H^a), 4.62 (d, J = 5.0 Hz 4H. H^d). ^{13}C NMR (100 MHz, chloroform-*d*) δ 154.70, 149.22, 137.33, 132.65, 122.26, 121.09, 118.49, 69.33. [**L1** + H]$^+$, calcd m/z =269.12, found m/z = 269.12. This compound was directly subjected to the next step of synthesis without further purification. A similar method was used to prepare ligands **L2–L4**.

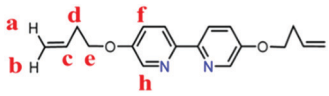

L2

Synthesis of ligand L2

Yield, 51%. ^{1}H NMR (500 MHz, DMSO-d_6) δ 8.32 (d, J = 2.8 Hz, 2H, H^h), 8.20 (d, J = 8.8 Hz, 2H, H^g), 7.48 (d, J = 11.6 Hz, 2H, H^f), 5.91 (brs, 2H, H^c), 5.21 (d, J = 17.2 Hz, 2H, H^b), 5.11 (d, J = 10.2 Hz, 2H, H^a), 4.15 (t, J = 6.6 Hz, 4H, H^e), 3.35 (s, 4H, H^d). ^{13}C NMR (100 MHz, chloroform-*d*) δ 149.11, 137.17, 134.09, 121.99, 121.08, 117.55, 67.81, 33.66. [**L2** + H]$^+$, calcd m/z =297.15, found m/z = 297.10. This compound was directly subjected to the next step of synthesis without further purification.

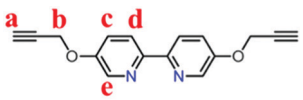

L3

Synthesis of ligand L3

Yield, 64%. ^{1}H NMR (500 MHz, chloroform-*d*) δ 8.39 (s, 2H, H^e), 8.27 (d, J = 8.8 Hz, 2H, H^d), 7.40 (d, J = 8.7 Hz, 2H, H^c), 7 4.78 (s, 4H, H^b), 2.57 (s, 2H, H^a). ^{13}C NMR (100 MHz, chloroform-*d*) δ 153.63, 149.63, 137.41, 122.47, 121.06, 77.80, 76.60, 56.26. [**L3** + H]$^+$, calcd m/z =265.28, found m/z = 265.10. This compound was directly subjected to the next step of synthesis without further purification.

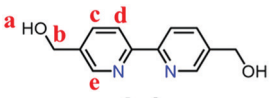

L4

Synthesis of ligand L4

The compound was synthesized by reference. ^{1}H NMR (400 MHz, DMSO-d_6) δ 8.60 (s, 2H, H^e), 8.34 (d, J = 8.1 Hz, 2H, H^d),

7.86 (d, J = 8.2 Hz, 2H, H^c), 5.40 (t, J = 5.7 Hz, 2H, H^a), 4.59 (d, J = 5.5 Hz, 4H, H^b).

Synthesis of the Cu(I)–POP complex C1

Ligand **L1** (20 mg, 0.074 mmol) and tetrafluoro–borate tetra(acetonitrile) copper (23 mg, 0.074 mmol) were dissolved in acetonitrile (3 mL) in an assembly tube and stirred at room temperature for 2 hours. Then, **L5** bis(2-diphenylphosphinophenyl)ether (40 mg, 0.074 mmol) was added and the mixture was stirred at room temperature for 8 hours. The solution was divided into three parts. It was grown by a solvent diffusion method with ethyl ether as the diffusion agent. A week later, the Cu(I)–POP complex **C1** was obtained. ^{1}H NMR (400 MHz, chloroform-d) δ 8.24 (d, J = 9.0 Hz, 2H, H^e), 7.82 (s, 2H, H^f), 7.46 (d, J = 11.7 Hz, 2H, H^d), 7.24 (m, 6H, $H^{j/k/m}$), 7.13 (m, 8H, H^i), 6.91 (m, 12H, $H^{g/h}$), 6.68 (m, 2H, H^l), 5.82 (m, 2H, H^b), 5.19 (m, 4H, H^a), 4.26 (d, J = 5.3 Hz, 4H, H^c). ^{13}C NMR (100 MHz, chloroform-d) δ 155.67, 144.88, 136.97, 134.38, 133.11, 132.08, 131.70, 130.71, 130.20, 128.83, 125.30, 124.09, 122.87, 120.41, 118.78, 69.39. [**C1**-BF_4^-]$^+$, calcd m/z = 868.93, found m/z = 868.90. Complexes **C2–C10** were prepared according to the same procedure as that used for **C1**.

Synthesis of the Cu(I)–POP complex C2

^{1}H NMR (400 MHz, chloroform-d) δ 8.24 (d, J = 9.0 Hz, 2H, H^f), 7.79 (s, 2H, H^g), 7.43 (d, J = 8.9 Hz, 2H, H^e), 7.24 (m, 6H, $H^{k/l/n}$), 7.13 (m, 8H, H^j), 6.94 (m, 12H, $H^{h/i}$), 6.67 (s, 2H, Hm), 5.69 (m, 2H, H^b), 5.05 (m, 4H, H^a), 3.72 (t, J = 6.6 Hz, 4H, H^d), 2.37 (m, 4H, H^c). ^{13}C NMR (100 MHz, chloroform-d) δ 158.10, 155.98, 144.84, 136.72, 134.41, 133.71, 133.17, 132.08, 130.72, 130.23, 128.85, 125.35, 123.97, 122.92, 120.39, 117.60, 68.00, 33.14. [**C2**-BF_4^-]$^+$, calcd m/z = 896.91, found m/z = 896.90.

Synthesis of the Cu(I)–POP complex C3

^{1}H NMR (400 MHz, chloroform-d) δ 8.32 (d, J = 9.0 Hz, 2H, H^d), 7.98 (s, 2H, H^e), 7.60 (d, J = 14.7 Hz, 2H, H^c), 7.30 (m, 6H, $H^{i/k/l}$), 7.18 (m, 8H, H^h), 7.02 (m, 12H, $H^{f/g}$), 6.72 (m, 2H, H^j), 4.49 (s, 2H, H^b), 2.42 (s, 2H, H^a). ^{13}C NMR (100 MHz, chloroform-d) δ 158.21, 154.78, 145.38, 137.17, 134.39, 133.07, 132.12, 130.26, 128.87, 125.28, 124.40, 123.06, 120.53, 78.48, 76.84, 56.57. [**C3**-BF_4^-]$^+$, calcd m/z = 865.28, found m/z = 865.17.

Synthesis of the Cu(I)–POP complex C4. ^{1}H NMR (400 MHz, acetonitrile-d_3) δ 8.26 (d, J = 8.0 Hz, 2H, H^d), 8.18 (s, 2H, H^e), 7.88 (d, J = 11.5 Hz, 2H, H^c), 7.26 (m, 6H, $H^{i/k/l}$), 7.14 (d, J = 9.4 Hz, 8H, H^h), 6.95 (m, 12H, $H^{f/g}$), 6.67 (m, 2H, H^j), 4.38 (d, J = 14.5 Hz, 4H, H^b), 3.48 (s, 2H, H^a). ^{13}C NMR (100 MHz, acetonitrile-d_3) δ 157.49, 149.79, 147.06, 139.19, 135.75, 133.46, 132.43, 131.47, 130.15, 129.40, 128.07, 124.45, 123.01, 121.14, 119.81, 116.40, 59.98. TOF-MS: fragment of **C4** with the formula [**C4**-L4-BF_4^-]$^+$, calcd m/z = 601.09, found m/z = 601.34.

Synthesis of the Cu(I)-DPPE complex C5

^{1}H NMR (500 MHz, DMSO-d_6) δ 8.76 (m, 2H^d), 8.46 (m, 2H^e), 8.21 (m, 2H^c), 7.46 (brs, 20H$^{f/g/h}$), 5.56 (m, 2H^a), 4.61 (m, 4H^b), 2.77 (s, 4H^i). ^{13}C NMR (100 MHz, DMSO-d_6) δ 150.86, 148.69, 141.14, 137.37, 132.70, 130.87, 129.61, 122.76, 60.43, 25.16. ERSI-MS: [**C5**-BF_4^-]$^+$, calcd m/z = 678.21, found m/z = 678.1.

Synthesis of the Cu(I)–DPPP complex C6

^{1}H NMR (500 MHz, DMSO-d_6) δ 8.66 (s, 4H$^{d/e}$), 8.15 (s, 2H^c), 7.41 (s, 4H^f), 7.32 (s, 16H$^{g/h}$), 5.57 (s, 2H^a), 4.61 (s, 4H^b), 2.84 (s, 4H^i), 2.20–1.99 (m, 2H^j). ^{13}C NMR (100 MHz, acetonitrile-d_3) δ 150.60, 148.53, 140.93, 137.14, 134.00, 132.25, 130.45, 129.29, 122.61, 60.40, 27.24, 19.48. ESI-MS: [**C6**-BF_4^-]$^+$, calcd m/z = 692.24, found m/z = 692.1.

Synthesis of the Cu(I)–Dppm complex C7

^{1}H NMR (400 MHz, acetonitrile-d_3) δ 7.82 (brs, 8H, $H^{f/g}$), 7.42 (d, J = 9.7 Hz, 4H, H^e), 7.23 (brs, 8H, H^h), 7.05 (brs, 32H, $H^{i/j}$), 6.01 (m, 4H, H^c), 5.31 (m, 8H, $H^{a/b}$), 4.55 (d, J = 7.5 Hz, 8H, H^d), 3.65 (s, 4H, H^k). ^{13}C NMR (100 MHz, chloroform-d) δ 155.52, 138.06, 132.42, 132.10, 130.04, 128.71, 123.79, 122.36, 118.52, 69.56. TOF-ESI-MS: fragment of **C7** with a formula of [**L1** + Cu + Dppm]$^+$, calcd m/z = 715.17, found m/z = 715.17.

Synthesis of the Cu(I)–Dppm complex C8

^{1}H NMR (400 MHz, acetonitrile-d_3) δ 7.79 (brs, 4H, H^g), 7.69 (s, 4H, H^h), 7.39 (d, J = 6.3 Hz, 4H, H^f), 7.24 (brs, 8H, H^i), 7.06 (brs, 32H, $H^{g/k}$), 5.93 (m, 4H, H^c), 5.19 (m, 8H, $H^{a/b}$), 4.00 (t, J = 9.5 Hz, 8H, H^e), 3.66 (s, 4H, H^l), 2.56 (m, 8H, H^d). ^{13}C NMR (100 MHz, acetonitrile-d_3) δ 156.76, 145.33, 138.73, 135.22, 133.22, 131.05, 123.79, 123.13, 117.88, 69.03, 33.93, 26.79. TOF-ESI-MS: fragment of **C8** with the formula [**L2** + Cu + Dppm]$^+$, calcd m/z = 743.20, found m/z = 743.19.

Synthesis of the Cu(I)–Dppm complex C9

^{1}H NMR (400 MHz, acetonitrile-d_3) δ 7.93 (brs, 2H, H^d), 7.79 (s, 2H, H^e), 7.50 (d, J = 13.4 Hz, 2H, H^c), 7.22 (brs, 4H, H^f), 7.03 (brs, 16H, $H^{g/h}$), 4.81 (s, 4H, H^b), 3.66 (s, 2H, H^a), 2.90 (s, 2H, H^i). ^{13}C NMR (100 MHz, acetonitrile-d_3) δ 155.47, 139.22, 133.20, 131.03, 129.46, 124.06, 123.13, 78.25, 57.44, 26.45. TOF-ESI-MS: [**C9**-BF_4^- + H_2O]$^+$, calcd m/z = 1528.32, found m/z = 1528.13.

Synthesis of the Cu(I)–Dppm complex C10

^{1}H NMR (400 MHz, acetonitrile-d_3) δ 8.09 (brs, 2H, H^d), 7.85 (brs, 4H, $H^{e/c}$), 7.19 (brs, 4H, H^f), 7.01 (brs, 16H, $H^{g/h}$), 5.07 (s, 2H, H^a), 4.56 (s, 4H, H^b), 3.71 (s, 2H, H^i). ^{13}C NMR (100 MHz, acetonitrile-d_3) δ 150.69, 139.13, 133.13, 130.53, 129.18, 62.23, 26.40. TOF-ESI-MS: [**C10**-BF_4^-]$^+$, calcd m/z = 1413.28 found m/z = 1413.07; [**C10**-BF_4^- + CH_3CH_2OH]$^+$, calcd m/z = 1459.32, found m/z = 1459.03.

Conflicts of interest

There are no conflicts to declare.

Acknowledgements

We thank the National Natural Science Foundation of China (No. 21971058, 21907063) for financial support and SSRF for

the crystal structure determination using synchrotron radiation X-ray diffraction analysis. This project was also supported by the Hubei Province Fund for Distinguished Young Scholars (2020CFA085), the research funds of ''Chu-Tian Distinguished Professor Scholar'' and the ''Hundred-Talent Program'' youth project (No. 430-090177) at Hubei University. We also thank the Natural Science Foundation of Guangdong Province (Grant No. 2019A1515010783), the Young Talents Program of Guangzhou University (Grant No. RQ2020080), and the Guangzhou Science and Technology Plan Project (Grant No. 202001010002).

References

1 D. R. McMillin and K. M. McNett, *Chem. Rev.*, 1998, **98**, 1201–1220.
2 N. Armaroli, *Chem. Soc. Rev.*, 2001, **30**, 113–124.
3 D. J. Casadonte and D. R. McMillin, *Inorg. Chem.*, 1987, **26**, 3950–3952.
4 D. R. McMillin, M. T. Buckner and B. T. Ahn, *Inorg. Chem.*, 1977, **16**, 943.
5 R. Jazzar, M. Soleilhavoup and G. Bertrand, *Chem. Rev.*, 2020, **120**, 4141–4168.
6 J. Zheng, Z. Lu, K. Wu, G.-H. Ning and D. Li, *Chem. Rev.*, 2020, **120**, 9675–9742.
7 S.-Y. Shi, M. C. Jung, C. Coburn, A. Tadle, D. S. M. Ravinson, P. I. Djurovich, S. R. Forrest and M. E. Thompson, *J. Am. Chem. Soc.*, 2019, **141**, 3576–3588.
8 G. Mani and V. Subramaniyan, in *Copper(I) Chemistry of Phosphines, Functionalized Phosphines and Phosphorus Heterocycles* ed. M. S. Balakrishna, Elsevier, 2019, pp. 237–258.
9 J. Y. Lin and K. Y. A. Lin, *Biomass Convers. Biorefin.*, 2019, **9**, 617–623.
10 R. Ilmi, J. I. Al Busaidi, A. Haque and M. S. Khan, *J. Coord. Chem.*, 2018, **71**, 3045–3076.
11 F. A. Watt, N. Dickmann, R. Schoch and S. Hohloch, *Inorg. Chem.*, 2020, **59**, 13621–13631.
12 M. Wallesch, M. Nieger, D. Volz and S. Brase, *Inorg. Chem. Commun.*, 2017, **86**, 232–240.
13 K. T. Mahmudov, A. V. Gurbanov, F. I. Guseinov, D. S. Guedes and M. C. Fatima, *Coord. Chem. Rev.*, 2019, **387**, 32–46.
14 M. Gernert, L. Balles-Wolf, F. Kerner, U. Müller, A. Schmiedel, M. Holzapfel, C. M. Marian, J. Pflaum, C. Lambert and A. Steffen, *J. Am. Chem. Soc.*, 2020, **142**, 8897–8909.
15 K. Rajabimoghadam, Y. Darwish, U. Bashir, D. Pitman, S. Eichelberger, M. A. Siegler, M. Swart and I. Garcia-Bosch, *J. Am. Chem. Soc.*, 2018, **140**, 16625–16634.
16 C. Marzano, *et al.*, Chapter 4 – Phosphine copper(I) complexes as anticancer agents: biological characterization. Part II. Copper(I) Chemistry of Phosphines, *Functionalized Phosphines and Phosphorus Heterocycles*, ed. M. S. Balakrishna, Elsevier, 2019, pp. 83–107.
17 Y. Zhang, M. Schulz, M. Wächtler, M. Karnahl and B. Dietzek, *Coord. Chem. Rev.*, 2018, **356**, 127–146.
18 Y. Chen, J. S. Chen, X. Gan and W. F. Fu, *Inorg. Chem. Acta*, 2009, **362**, 2492–2498.
19 Y. Zhang, M. Schulz, M. Waechtler, M. Karnahl and B. Dietzek, *Coord. Chem. Rev.*, 2018, **356**, 127–146.
20 H. Ke, L. P. Yang, M. Xie, Z. Chen, H. Yao and W. Jiang, *Nat. Chem.*, 2019, **11**, 470–477.
21 S. Shanmuganathan, C. Schulzke, P. G. Jones and J. W. Heinicke, *J. Organomet. Chem.*, 2020, **926**, 121487.
22 X. F. Jiang, F. K. Hau, Q. F. Sun, S. Y. Yu and V. W. Yam, *J. Am. Chem. Soc.*, 2014, **136**, 10921–10929.
23 X. X. Jin, T. Li, D. P. Shi, L. J. Luo, Q. Q. Su, J. Xiang, H. B. Xu, C. F. Leung and M. H. Zeng, *New J. Chem.*, 2020, **44**, 13393–13400.
24 L. H. He, Y. S. Luo, B. S. Di, J. L. Chen, C. L. Ho, H. R. Wen, S. J. Liu, J. Y. Wang and W. Y. Wong, *Inorg. Chem.*, 2017, **56**, 10311–10324.
25 F. Yu, Y. Sheng, D. Wu, K. Qin, H. Li, G. Xie, Q. Xue, Z. Sun, Z. Lu, H. Ma and X. C. Hang, *Inorg. Chem.*, 2020, **59**, 14493–14500.
26 J.-H. Jia, D. Liang, R. Yu, X.-L. Chen, L. Meng, J.-F. Chang, J.-Z. Liao, M. Yang, X.-N. Li and C.-Z. Lu, *Chem. Mater.*, 2019, **32**, 620–629.
27 P. Zhang, Y. Wang, W. Huang, Z. Zhao, H. Li, H. Wang, C. He, J. Liu and Q. Zhang, *Sens. Actuators, B*, 2018, **255**, 283–289.
28 C. L. Wang, D. Ikhlef, S. Kahlal, J. Y. Saillard and D. Astruc, *Coord. Chem. Rev.*, 2016, **316**, 1–20.
29 A. Anamika, A. K. Agrahari, K. K. Manar, C. L. Yadav, V. K. Tiwari, M. G. B. Drew and N. Singh, *New J. Chem.*, 2019, **43**, 8939–8949.
30 C. Iacobucci, S. Reale, J.-F. Gal and F. D. Angelis, *Angew. Chem., Int. Ed.*, 2015, **54**, 3065–3068.
31 C. Wang, D. Wang, S. Yu, T. Cornilleau, J. Ruiz, L. Salmon and D. Astruc, *ACS Catal.*, 2016, **6**, 5424–5431.
32 A. Beltran, I. Gata, C. Maya, J. Avo, J. C. Lima, C. A. T. Laia, R. Peloso, M. Outis and M. C. Nicasio, *Inorg. Chem.*, 2020, **59**, 10894–10906.
33 D. Khalili, R. Evazi, A. Neshat, J. Aboonajmi and F. Osanlou, *Inorg. Chim. Acta*, 2020, **506**, 119470.
34 J. S. S. Neto and G. Zeni, *Coord. Chem. Rev.*, 2020, **409**, 213217.
35 C. Wang, D. Ikhlef, S. Kahlal, J.-Y. Saillard and D. Astruc, *Coord. Chem. Rev.*, 2016, **316**, 1–20.

